Vibro-acoustic analysis of orthotropic sound radiating plate using a simple first-order shear deformation theory

T.Y. Kam, A. Nayan*
Mechanical Engineering Department,
National Chiao Tung University,
Hsin Chu 300, Taiwan
*Email: anayan@gmail.com

Abstract

A simple first-order shear deformation theory is presented for vibro-acoustic analysis of sound radiating plate by reducing one unknown displacement function. The proposed method is formulated based on the Rayleigh-Ritz method for natural frequency and mode shape analysis and the first Rayleigh integral for sound pressure level (SPL) curve prediction. The numerical solution of SPL curve prediction obtained using this method is compared with that obtained using the other existing theory. The comparison study shows that the simple method can produce results close to those produced by the existing theory. The applications of the proposed method have been illustrated by determining the SPL curves of plates with different thicknesses.

Keywords: Vibro-acoustic, simple FSDT, Rayleigh-Ritz method, sound radiation.

1. Introduction

Vibro-acoustic is one of structure which widely used in different industries such as aircraft, automobile, medical, and sound system industries. Especially for audio industry, the most prominent effort is to fabricate the speaker that able to produce good sound quality and also simple assembly.

Many researchers have been developing of methods to investigate and analyze structure that yield optimal design. Using orthotropic material such as balsa wood is one solution since this material has low density property and good stiffness [1-5]. The optimal design obtained is not regardless of effectiveness the analysis method chosen. Classical Plate Theory (CPT) is common approach where it ignore the effect of shear deformation and this method only suitable for thin plate structure [6-8]. First-Order Shear Deformation Theory (FSDT) is another method introduced by Reissner [9] and Mindlin [10] and adopted by Kam [11-12]. A simple FSDT have been developed by Thai [13-14] for bending and vibration analysis of laminate plate.

In this paper, the simple approach is adopted together with Rayleigh-Ritz method and the first Rayleigh integral to analyze vibro-acoustic behaviors and construct SPL curves on single layer orthotropic balsa wood material. Effectiveness of this approach will be compared with previous result [15] using normal FSDT.

2. Plate vibration analysis

The orthotropic sound radiation plate geometrically has size a (length) x b (width) x h_p (thickness) with $a \leq b$. It has boundary condition elastically strained along the plate periphery with translational and rotational spring constant intensities K_{Li} and K_{Ri}, respectively as shown in Fig. 1. A simple first-order shear deformation theory is used to model the displacements of the plate and stiffeners. By simplifying assumptions on existing FSDT, some unknown variable are reduced. The displacement field of the plate based on existing FSDT is expressed as

$$\begin{aligned} u_p &= u_{op}(x,y,t) + z_p\theta_{xp}(x,y,t) \\ v_p &= v_{op}(x,y,t) + z_p\theta_{yp}(x,y,t) \\ w_p &= w_{op}(x,y,t) \end{aligned} \tag{1}$$

where u_p, v_p, and w_p are the displacements in *x, y,* and *z* directions, respectively; u_{op}, v_{op}, w_{op}, θ_{xp}, θ_{yp} are five unknown displacements function of the mid-plane of plate. The transverse displacement w_p divides into bending w_B and shear w_S parts. Assuming that $\theta_{xp} = -\frac{\partial w_B}{\partial x}$ and $\theta_{yp} = -\frac{\partial w_B}{\partial y}$ yields to change of the displacement field for new theory as

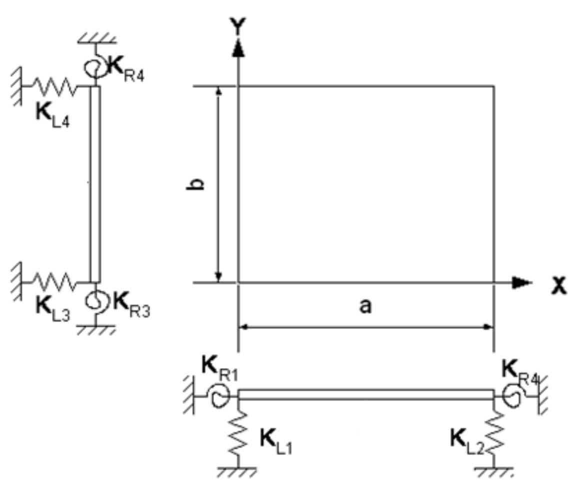

Fig. 1 Orthotropic sound radiation plate

$$u_p = u_{op}(x,y,t) - z_p \frac{\partial w_B}{\partial x}(x,y,t)$$
$$v_p = v_{op}(x,y,t) - z_p \frac{\partial w_B}{\partial y}(x,y,t) \quad (2)$$
$$w_p = w_B(x,y,t) + w_S(x,y,t)$$

Clearly shown the unknown of displacement function remains only four (u_{op}, v_{op}, w_B, w_S). The strain-displacement relations of the plate are expressed as

$$\varepsilon_x = \frac{\partial u_{op}}{\partial x} - z_p \frac{\partial^2 w_B}{\partial x^2}$$
$$\varepsilon_y = \frac{\partial u_{op}}{\partial y} - z_p \frac{\partial^2 w_B}{\partial y^2}$$
$$\gamma_{xy} = \frac{\partial u_{op}}{\partial y} + \frac{\partial v_{op}}{\partial x} - 2z_p \frac{\partial^2 w_B}{\partial x \partial y} \quad (3)$$
$$\gamma_{xz} = \frac{\partial w_S}{\partial x}$$
$$\gamma_{yz} = \frac{\partial w_S}{\partial y}$$

The stress-strain relations of the orthotropic plate are given as [16]

$$\begin{Bmatrix} \sigma_x \\ \sigma_y \\ \tau_{yz} \\ \tau_{xz} \\ \tau_{xy} \end{Bmatrix} = \begin{bmatrix} Q_{11} & Q_{12} & 0 & 0 & 0 \\ Q_{12} & Q_{22} & 0 & 0 & 0 \\ 0 & 0 & Q_{44} & 0 & 0 \\ 0 & 0 & 0 & Q_{55} & 0 \\ 0 & 0 & 0 & 0 & Q_{66} \end{bmatrix} \begin{Bmatrix} \varepsilon_x \\ \varepsilon_y \\ \gamma_{yz} \\ \gamma_{xz} \\ \gamma_{xy} \end{Bmatrix} \quad (4)$$

with

$$Q_{11} = \frac{E_1}{1-\nu_{12}\nu_{21}}$$
$$Q_{12} = \frac{\nu_{12}E_2}{1-\nu_{12}\nu_{21}}$$
$$Q_{22} = \frac{E_2}{1-\nu_{12}\nu_{21}} \quad (5)$$
$$Q_{44} = G_{23}$$
$$Q_{55} = G_{13} = G_{12}$$
$$Q_{66} = G_{12}$$

Where Q_{ij} is reduce stiffness constant, E_i isYoung's modulus in the *i*th direction, ν_{12} is Poisson ratio, G_{ij} is shear modulus.

The strain energy, U_p, of the plate is

$$U_p = \frac{1}{2}\int_{V_p} \left(\sigma_x\varepsilon_x + \sigma_y\varepsilon_y + 2\tau_{xy}\varepsilon_{xy} + 2\tau_{xz}\varepsilon_{xz} + 2\tau_{yz}\varepsilon_{yz}\right) dV_p \quad (6)$$

Using the relations in Eqs. (1)-(4) and integration through the plate thickness, Eq. (6) can be rewritten as

$$\begin{aligned} U_p = \frac{1}{2}\int_0^a \int_0^b \Bigg[& Q_{11}h_p\left(\frac{\partial u}{\partial x}\right)^2 + Q_{11}\frac{{h_p}^3}{12}\left(\frac{\partial^2 w_B}{\partial x^2}\right)^2 \\ & + 2Q_{12}h_p\left(\frac{\partial u}{\partial x}\right)\left(\frac{\partial v}{\partial y}\right) \\ & + 2Q_{12}\frac{{h_p}^3}{12}\left(\frac{\partial^2 w_B}{\partial x^2}\right)\left(\frac{\partial^2 w_B}{\partial y^2}\right) + Q_{22}h_p\left(\frac{\partial v}{\partial y}\right)^2 \\ & + Q_{22}\frac{{h_p}^3}{12}\left(\frac{\partial^2 w_B}{\partial y^2}\right)^2 \\ & + 2Q_{66}h_pK_p\left(\frac{\partial u}{\partial y}\right)\left(\frac{\partial v}{\partial x}\right) \\ & + Q_{66}h_pK_p\left(\frac{\partial u}{\partial y}\right)^2 \\ & + Q_{66}h_pK_p\left(\frac{\partial v}{\partial x}\right)^2 \\ & + Q_{66}K_p\frac{{h_p}^3}{3}\left(\frac{\partial^2 w_B}{\partial x \partial y}\right)^2 \\ & + Q_{55}h_pK_p\left(\frac{\partial w_S}{\partial x}\right)^2 \\ & + Q_{44}h_pK_p\left(\frac{\partial w_S}{\partial y}\right)^2 \Bigg] dydx \end{aligned} \quad (7)$$

where K_p is shear correction factor.

The kinetic energy, T_p of the plate is

$$T_p = \frac{1}{2}\int_{V_p} \rho_p\left(\dot{u}_p^2 + \dot{v}_p^2 + \dot{w}_p^2\right) dV_p \quad (8)$$

Refer to Eq. (1), this equation can be rewritten as

$$\begin{aligned} T_p = \frac{1}{2}\int_0^b \int_0^a \rho_p \Bigg[& h_p\left(\frac{\partial u_{op}}{\partial t}\right)^2 \\ & + h_p\left(\frac{\partial v_{op}}{\partial t}\right)^2 \\ & + h_p\left(\frac{\partial w_B}{\partial t}\right)^2 + h_p\left(\frac{\partial w_S}{\partial t}\right)^2 \\ & + 2h_p\left(\frac{\partial w_B}{\partial t}\right)\left(\frac{\partial w_S}{\partial t}\right) \\ & + \frac{{h_p}^3}{12}\left(\frac{\partial^2 w_B}{\partial t \partial x}\right)^2 \\ & + \frac{{h_p}^3}{12}\left(\frac{\partial^2 w_B}{\partial t \partial y}\right)^2 \Bigg] dxdy \end{aligned} \quad (9)$$

The strain energy store, U_s, stored in the elastic restraints is written as

$$\begin{aligned} U_s = & \frac{K_{L1}}{2}\int_0^b w^2\Big|_{x=0} dy \\ & + \frac{K_{L2}}{2}\int_0^b w^2\Big|_{x=a} dy \\ & + \frac{K_{L3}}{2}\int_0^a w^2\Big|_{y=0} dx \\ & + \frac{K_{L4}}{2}\int_0^a w^2\Big|_{y=b} dx \end{aligned}$$

$$+\frac{K_{R1}}{2}\int_0^b \left(\frac{\partial w}{\partial x}\right)^2\Big|_{x=0} dy + \frac{K_{R2}}{2}\int_0^b \left(\frac{\partial w}{\partial x}\right)^2\Big|_{x=a} dy + \frac{K_{R3}}{2}\int_0^a \left(\frac{\partial w}{\partial y}\right)^2\Big|_{y=0} dx + \frac{K_{R4}}{2}\int_0^a \left(\frac{\partial w}{\partial y}\right)^2\Big|_{y=b} dx \quad (10)$$

The total strain energy U of the elastically restrained orthotropic plate are written as

$$U = U_p + U_S \quad (11)$$

Free vibration of the elastically restrained orthotropic plate is solved by the Rayleigh-Ritz method. Thus, the displacement of plate are expressed as

$$\begin{aligned} u_{0p}(x,y,t) &= U(x,y)\sin\omega t \\ v_{0p}(x,y,t) &= V(x,y)\sin\omega t \\ w_B(x,y,t) &= W_B(x,y)\sin\omega t \\ w_S(x,y,t) &= W_S(x,y)\sin\omega t \end{aligned} \quad (12)$$

With

$$\begin{aligned} U(\xi,\eta) &= \sum_{i=1}^{\hat{A}}\sum_{j=1}^{\hat{B}} C_{ij}\phi_i(\xi)\psi_j(\eta) \\ V(\xi,\eta) &= \sum_{i=1+\hat{A}}^{\hat{C}}\sum_{j=1+\hat{B}}^{\hat{D}} C_{ij}\phi_i(\xi)\psi_j(\eta) \\ W_B(\xi,\eta) &= \sum_{i=1+\hat{C}}^{\hat{I}}\sum_{j=1+\hat{D}}^{\hat{J}} C_{ij}\phi_i(\xi)\psi_j(\eta) \\ W_S(\xi,\eta) &= \sum_{i=1+\hat{I}}^{\hat{M}}\sum_{j=1+\hat{J}}^{\hat{N}} C_{ij}\phi_i(\xi)\psi_j(\eta) \end{aligned} \quad (13)$$

where C_{ij} are unknown constants; $\hat{A},\hat{B},\hat{C},\hat{D},\hat{I},\hat{J},\hat{M},\hat{N}$ denote the numbers of terms in the series. Legendre's polynomials are used to represent the characteristic functions, ϕ and ψ. Let $\xi = \frac{2x}{a} - 1$ and $\eta = \frac{2y}{b} - 1$. The normalized characteristic functions, for instance, $\phi_c(\xi)$, are given as

$$\begin{aligned} &\phi_1(\xi) = 1 \\ &\phi_2(\xi) = \xi, \qquad -1 \le \xi \le 1 \\ &\text{For } n \ge 3, \\ &\phi_n(\xi) = [(2n-3)\xi \times \phi_{n-1}(\xi) - (n-2) \times \phi_{n-2}(\xi)]/(n-1) \end{aligned} \quad (14)$$

With the satisfaction of the following orthogonally condition:

$$\int_{-1}^{1}\phi_n(\xi)\phi_m(\xi)d\xi = \begin{cases} 0, & if\ n \ne m \\ 2/2n-1, & f\ n = m \end{cases} \quad (15)$$

The extremization of the function $\Pi = U - T$ gives the following eigenvalue problem.

$$[\boldsymbol{K} - \boldsymbol{\omega}^2\boldsymbol{M}]\boldsymbol{C} = \mathbf{0} \quad (16)$$

Where $\boldsymbol{K}$ and $\boldsymbol{M}$ are structure stiffness and mass matrices; $\boldsymbol{\omega}$ is circular frequency. The natural frequency and mode shape of the orthotropic plate can be determined by solving above eigenvalue problem. The terms in **K** and **M** are listed in the appendix

3. Plate sound radiation analysis

A variational approach is used to derive the equation of motion for sound radiation plate panel subjected to forced vibration. The panel excited by an electro-magnetic transducer with a cylindrical voice coil, the harmonic driving force $F(t) = F_o \sin\omega t$ is distributed uniformly around the periphery of the voice coil. The amplitude of harmonic force is $F_o = BLI$ with B = magnetic flux, L = wire length, and I = electric current. The equation of motion can be expressed as

$$\underline{\boldsymbol{M}\ddot{\boldsymbol{C}}} + \underline{\boldsymbol{D}\dot{\boldsymbol{C}}} + \underline{\boldsymbol{K}\boldsymbol{C}} = \underline{\boldsymbol{F}} \quad (17)$$

Where $\boldsymbol{F}$ is force vector containing the following terms

$$\begin{aligned} F_{mn} &= \frac{F_o}{2\pi r_c}\int_0^{2\pi}\phi_m\left(\frac{2r_c}{a}\cos\theta\right)\varphi_n\left(\frac{2r_c}{b}\cos\theta\right)d\theta\sin\omega t, \\ &\text{for } m = 1+\hat{I},\ldots,\hat{M}; n = 1+\hat{J},\ldots,\hat{N} \\ &= 0\ for\ other\ i,j \end{aligned} \quad (18)$$

The damping matrix **D** is

$$[\mathbf{D}] = \alpha[\mathbf{M}] + \beta[\mathbf{K}] \quad (19)$$

with $\alpha = \zeta\omega$, $\beta = 2\zeta/\omega$ where ζ is damping ratio at the first resonance frequency of elastically restrained plate. Eq. (19) can be solved using the modal analysis method.

The vibration on the baffled plate with area S shown in Fig. 2 creates the sound pressure $p(r,t)$. This can be determined using the first Rayleigh integral.

$$p(r,t) = \frac{-\varpi^2\rho_0}{2\pi}\sum_i A_i e^{j(2\varpi t + \theta_i - kR_i)}\frac{\Delta S_i}{R_i} \quad (20)$$

where ρ_0 is air density; k is wave number $(=\varpi/c)$ with c being speed of sound; r_p is the distance between the plate center and the point of measurement; $R_i = |r_p - r_i|$ the distance between the observation point and the position of the surface element at r_i; θ is phase angle; $j = \sqrt{-1}$. For air at 20 ^oC and standard atmospheric pressure, $\rho_0 =$ 1.2kg/m^3 and c = 344 m/s. The SPL produced by the plate is calculated as

$$SPL \equiv 20\log_{10}\left(\frac{p_{rms}}{2\times 10^{-5}}\right)dB \quad (21)$$

with

$$p_{rms} = \left[\frac{1}{T}\int_{-T/2}^{T/2}|p(r,t)|^2 dt\right]^{\frac{1}{2}} \quad (22)$$

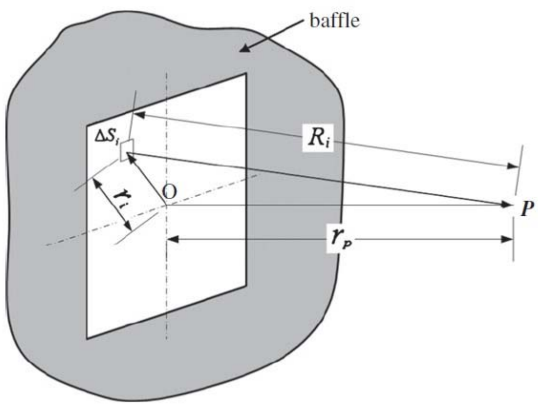

Fig. 2 Sound pressure measurement on baffle plate

4. Result validation and discussion

The simple FSDT method is applied to analyze the vibro-acoustic behavior of orthotropic sound radiation plate of size 26.5 mm × 20.5 mm × 1 mm. The plate is elastically restrained along periphery and trasversely loaded 0.58415 N uniformly distribute on 9.35 mm radius in the middle of plate as exciter. The properties of the plate, spring constant intensity of the surround spring material are listed in Table 1.

The first step to validate the method proposed in this paper, the plate is modeled by three methods; Finite element code ANSYS, FSDT, and simple FSDT. Using shell99 element type in ANSYS, plate is modeled to determine five natural frequency and mode shape as basic comparison purpose.

Table 1 Properties of orthotropic plate

Material constants	**Plate**	**Surround**
E_1 (GPa)	3.7	
E_2 (GPa)	0.055	
ν_{12}	0.03	
ν_{23}	0.2	
ν_{13}	0.03	
G_{12} (GPa)	0.05	
G_{23} (GPa)	0.05/6	
G_{13} (GPa)	0.05	
ρ (kg/m^3)	300	
K_L (N/m^2)		4744.7
K_R (N)		0

In FSDT and simple FSDT, the five natural frequencies and mode shape are derived using Rayleigh-Ritz method with 10 terms characteristic function of displacement. The results of numerically solution shown in Table 2 are close agreement between three methods. Both existing FSDT and simple FSDT shown the discrepancy with finite element method are less than 1%. The largest percentage discrepancy about 2.88% occurs on fourth natural frequency of simple FSDT method.

The sound radiation on orthotropic plate is next observation. The SPL curves of three methods shown in Fig. 3 for comparison are almost exactly same, especially between 20 Hz and 4 kHz. The curves dip and rise along 1.5 kHz because of plate stiffness, the stiffer of the plate the better curve will be created.

Table 2 Mode shape and natural frequency of orthotropic sound radiating plate

Mode shape no.	Methods		
	ANSYS	FSDT [15]	Simple FSDT
1		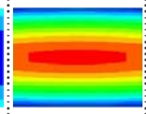	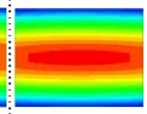
NF (Hz)	354.80	354.6	354.9
D (%)		0.06	0.03
2		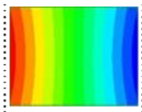	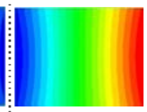
NF (Hz)	511.5	509.9	510.8
D (%)		0.31	0.14
3	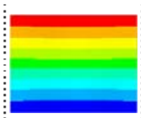	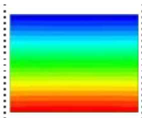	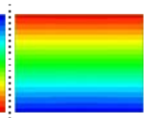
NF (Hz)	541.12	541.2	542.4
D (%)		0.01	0.24
4			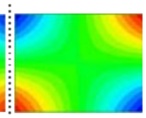
NF (Hz)	1073.4	1071	1100
D (%)		0.22	2.48
5	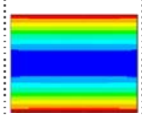	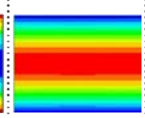	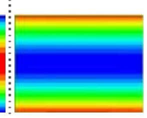
NF (Hz)	1339.2	1333	1351
D (%)		0.47	0.88

*) NF = Natural Frequency
D = Difference

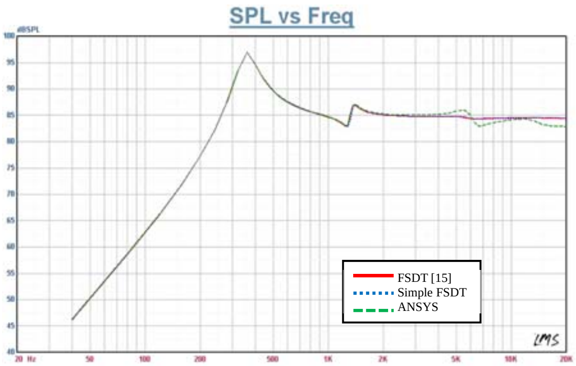

Fig. 3 SPL curve of orthotropic plate (h = 1 mm) with three methods analysis

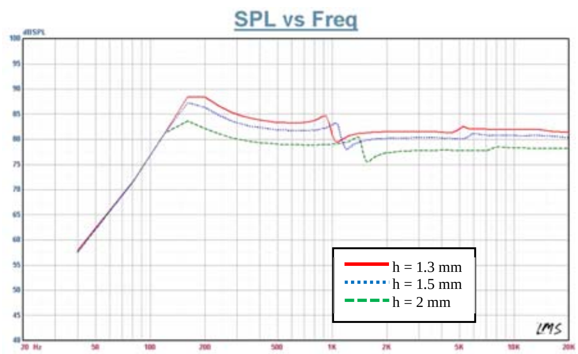

Fig. 4 SPL curve of orthotropic plate with different thickness (h) and plate ratio a/b = 2.92

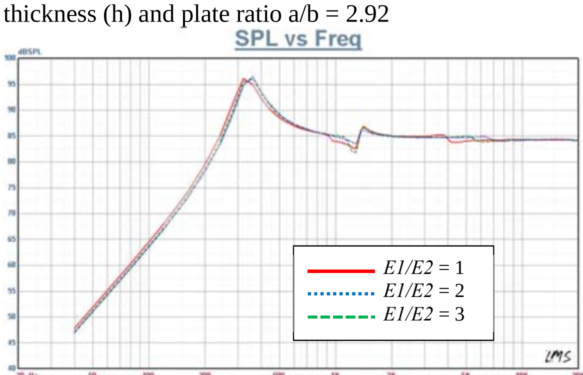

Fig 5 SPL curve of orthotropic plate with E1/E2 (a/b = 1.25, E2 = 0.055 GPa)

The next step of proving the proposed method in this paper to ensure it suitable for vibro-acustic orthotropic plate analysis, some modification of plate properties are made and analyzed. The plate ratio *a/b* = 2.92 with *a* = 76 *mm*, *b* = 26 *mm* and several different thickness (h_p) 1.3 mm, 1.5 mm, and 2 mm are used to analyze the plate thickness plate ratio effect and SPL curve behavior. Fig. 4 clearly shows the thickness of plate directly affect the magnitude of SPL curve, the thicker of plate sound radiation the lower sound radiation created. On the other hand, the thickness of plate also yield its stiffness. It is shown rise and dip of SPL curve around 1 kHz, where the rise and dip curve of the thinnest plate (1.3 mm) occurs below 1 kHz while the others two it shift to higher than 1 kHz. Consequently, the SPL magnitude will decrease in line with increasing the thickness and weight of plate.

Finally, the effects of the ratio of the plate Young's moduli (E1/E2) on the SPL curve of are studied. Setting E2 = 0.055GPa, the SPL curves for E1/E2 = 1, 2, and 3 are shown in Fig. 5 for comparison. The small variations of the SPL curves in some frequencies for these cases have demonstrated the fact that E1/E2 has negligible effects on the SPL curve behavior

5. Conclusions

Simple FSDT approach is adopted to analyze the vibro-acoustic of orthotropic sound radiating plate. The equations is derived with Rayleigh-Ritz method for natural frequency and mode shape analysis and the first Rayleigh integral for SPL curves. Validation studies show that reducing one variable on existing FSDT yield the prediction close each other. In conclusion, the present simple FSDT method proposed show the accuracy of predicting the natural frequency, mode shape, and SPL curve of orthotropic sound radiating plate close to existing theory.

6. Acknowledgements

This work was supported by the National Science Council Grant No.: NSC 102-2623-E-009-005.

7. References

1. Franco F, De Rosa S, Polito T. Finite element investigations on the vibro- acoustic performance of plane plates with random stiffness. Mech Adv Mater Struct 2011; 18(7): 484-97.
2. Sorokin SV. Vibrations of and sound radiation from sandwich plates in heavy fluid loading conditions. Compos Struct 2000; 48: 219–30.
3. Cao X, Hua H, Zhang Z. Sound radiation from shear deformable stiffened laminated plates. J Sound Vib 2011; 330 (16): 4047–63.
4. Zhang X, Li WL. A unified approach for predicting sound radiation from baffle rectangular plates with arbitrary boundary. J Sound Vib 2010; 329 (25): 5307–20
5. Li S. Active modal control simulation of vibro-acoustic response of a fluid-loaded plate. J Sound Vib 2011; 330 (23): 5545–57
6. Bui TQ, Nguyen MN, Zhang C. An efficient meshfree method for vibration analysis of laminated composite plates. Comput Mech 2011; 48(2): 175–93.
7. Shojaee S, Valizadeh N, Izadpanah E, Bui T, Vu T-V. Free vibration and buckling analysis of laminated composite plates using the NURBS-based isogeometric finite element method. Compos Struct

2012; 94(5): 1677–93.
8. Whitney JM, Leissa AW. Analysis of heterogeneous anisotropic plates. J Appl Mech 1969; 36(2): 261–6.
9. Reissner E. The effect of transverse shear deformation on the bending of elastic plates. J Appl Mech 1945; 12(2): 69–72.
10. Mindlin RD. Influence of rotatory inertia and shear on flexural motions of isotropic, elastic plates. J Appl Mech 1951; 18(1): 31–8.
11. Kam TY, Jiang CH, Lee BY. Vibro-acoustic formulation of elastically restrained shear deformable stiffened rectangular plate. J Compos Struct 2012; 94: 3132–41.
12. Jiang CH, Chang YH, Kam TY, Optimal design of rectangular composite flat-panel sound radiators considering excitation location. J Compos Struct 2014; 108: 65–76.
13. Thai HT, Choi DH. A simple first-order shear deformation theory for the bending and free vibration analysis of functionally graded plates. Compos Struct 2013; 101: 332–40.
14. Thai HT, Choi DH. A simple first-order shear deformation theory for laminated composite plates. Compos Struct 2013; 101: 332–40.
15. Li BY, Vibration and Sound Radiation of Laminated Composite Plates Considering the Effects of Shear Deformation and Attached Masses. National Ciao Tung University, Department of Mechanical Engineering, Hsinchu, 2011.
16. Jones RM. Mechanics of composite material. New York: McGraw-Hill Inc.; 1975.

Appendix

$$\left(\begin{bmatrix} K_{11} & 0 & 0 & 0 \\ 0 & K_{22} & 0 & 0 \\ 0 & 0 & K_{33} & K_{34} \\ 0 & 0 & K_{43} & K_{44} \end{bmatrix} - \omega^2 \begin{bmatrix} M_{11} & 0 & 0 & 0 \\ 0 & M_{22} & 0 & 0 \\ 0 & 0 & M_{33} & 0 \\ 0 & 0 & 0 & M_{44} \end{bmatrix}\right)\begin{Bmatrix} C_{ij} \\ C_{mn} \\ C_{ab} \\ C_{cd} \end{Bmatrix} = \begin{Bmatrix} 0 \\ 0 \\ 0 \\ 0 \end{Bmatrix} \quad \text{(A1)}$$

$$\begin{aligned}
\left[K^{11}\right]_{ij\bar{i}\bar{j}} = \frac{1}{2}\Big[& Q_{11}\frac{{h_p}^3}{3}\frac{2b}{a^3}E^{22}F^{00} + 2Q_{12}\frac{{h_p}^3}{3}\frac{1}{ab}\left(E^{20}F^{02} + E^{02}F^{20}\right) \\
& + Q_{22}\frac{{h_p}^3}{3}\frac{2a}{b^3}E^{00}F^{22} + Q_{66}K_p\frac{{h_p}^3}{3}\frac{8}{ab}E^{11}F^{11}\Big] \\
& + \frac{1}{2}\left[K_{L_1}bF^{00}BB^{00} + K_{L_2}bF^{00}BB^{00} + K_{L_3}aE^{00}BB^{00} + K_{L_4}aE^{00}BB^{00}\right] \\
& + K_C E^{00}F^{00}
\end{aligned} \quad \text{(A2)}$$

$$\left[K^{22}\right]_{mn\bar{m}\bar{n}} = \frac{1}{2}\left[Q_{55}K_p h_p\frac{2b}{a}E^{11}F^{00} + Q_{44}K_p h_p\frac{2a}{b}E^{00}F^{11}\right]$$

$$\left[K^{33}\right]_{ab\bar{a}\bar{b}} = \frac{1}{2}\left[Q_{11}h_p\frac{2b}{a}E^{11}F^{00} + Q_{66}K_p h_p\frac{2a}{b}E^{00}F^{11}\right]$$

$$\left[K^{34}\right]_{abcd} = \frac{1}{2}\left[2Q_{12}h_p E^{01}F^{10} + 2Q_{66}K_p h_p E^{10}F^{01}\right]$$

$$\left[K^{44}\right]_{cd\bar{c}\bar{d}} = \frac{1}{2}\left[Q_{22}h_p\frac{2a}{b}E^{00}F^{11} + Q_{66}K_p h_p\frac{2b}{a}E^{11}F^{00}\right]$$

and

$$\begin{aligned}
\left[M^{11}\right]_{ij\bar{i}\bar{j}} &= \rho_p h_p^3\frac{b}{12a}E^{10}F^{00} + \rho_p h_p^3\frac{a}{12b}E^{00}F^{10} + \rho_p h_p^3\frac{ab}{4}E^{00}F^{00} \\
\left[M^{22}\right]_{mn\bar{m}\bar{n}} &= \rho_p h_p\frac{ab}{4}E^{00}F^{00} \\
\left[M^{33}\right]_{ab\bar{a}\bar{b}} &= \rho_p h_p\frac{ab}{4}E^{00}F^{00} \\
\left[M^{44}\right]_{cd\bar{c}\bar{d}} &= \rho_p h_p\frac{ab}{4}E^{00}F^{00}
\end{aligned} \quad \text{(A3)}$$

where

$$\begin{aligned}
& r, s = 0,1; \\
& i, j, \bar{i}, \bar{j} = 1,2,3,\cdots I, J \\
& m, n, \bar{m}, \bar{n} = 1,2,3,\cdots M, N \\
& a, b, \bar{a}, \bar{b} = 1,2,3,\cdots A, B \\
& c, d, \bar{c}, \bar{d} = 1,2,3,\cdots C, D \\
& E_{im}^{rs} = \int_{-1}^{1}\left[\frac{d^r\phi(\xi)}{d\xi^r}\frac{d^s\phi(\xi)}{d\xi^s}\right]d\xi \\
& F_{jn}^{rs} = \int_{-1}^{1}\left[\frac{d^r\psi(\eta)}{d\eta^r}\frac{d^s\psi(\eta)}{d\eta^s}\right]d\eta
\end{aligned} \quad \text{(A4)}$$